
Multi-variable Optimization Formulation for Maximum Power Transmission Capability of a Standalone Six-phase Induction Generator

Saikat Ghosh* and S. N. Mahato

Dept. of Electrical Engineering, NIT Durgapur, 713209, India

E-mail: saikatghosh1407@gmail.com; sankar.mahato@ee.nitdgp.ac.in

**Corresponding Author*

Received 31 July 2021; Accepted 22 November 2021;

Publication 16 February 2022

Abstract

This paper presents an optimization based scheme to derive the maximum power transmission capability of a self-excited six-phase induction generator (SPIG). For execution of this proposed scheme, an easy and straight forward method has been developed here for figuring out the maximum amount of power which can be transmitted by SPIG considering different functional conditions. An optimization based problem is formulated with the help of multi-variable constraint, for finding out the maximum power transmission capability of SPIG. The total impedance of SPIG, calculated from its equivalent circuit, is considered as the objective function. Fmincon optimization toolbox of MATLAB has been used to solve this numerical based problem. The critical power and the maximum power transmission capability have been investigated for variations of capacitor, load power factor and speed. The power transmission capability of SPIG directly depends on the factors like machine parameters, rotor speed, power factor of the load and the capacitance

Distributed Generation & Alternative Energy Journal, Vol. 37_3, 683–702.

doi: 10.13052/dgaej2156-3306.37314

© 2022 River Publishers

value of self-excitation. From the analysis of the simulated results, it is found that the performance of SPIG is satisfactory for various operating conditions.

Keywords: Six-phase induction generator, excitation capacitor, renewable energy sources, optimization, maximum power transmission, rural area electrification.

1 Introduction

Presently, our earth is encountered by two major problems, which are energy crisis and pollution. Higher uses of renewable energy like small hydro, wind and solar is the best and probably the single solution to this problem. It is known to everyone that renewable energy resources have several advantages over conventional energy resources [1, 2]. Till now, one fifth of the entire world population has no access to electricity because of their remote location where the national grid is unavailable. But the interesting thing is that 80% of this remote area has huge availability of non-conventional energy resources. Hence, the development of small-scale power generating system using these renewable energy sources is the best solution for electrification of this kind of remote un-electrified area [3, 4]. The SPIG may be used in such systems because of its easy availability, little maintenance and low cost.

Now a days, a lot of research is going on multi-phase induction generator (more than three phases in stator) because of its several advantages over conventional three-phase induction generator like increased total power rating keeping per phase power rating same as previous, higher fault tolerance capability and less torque ripple [5]. SPIG is a special type of multi-phase induction generator; where two different three-phase windings are placed inside of its stator which are electrically isolated from each other but magnetically coupled as they are placed in same slots of the stator. As the total power generation is subdivided into two winding sets, this proposed system allows the uses of power electronic switches of lower rating. One of the major advantages of this configuration is that the fault tolerance capability is very high. If the fault occurs at any three-phase set out of six-phases, then the SPIG is still capable to supply power to load with lower power rating [6, 7]. Nounou et al. [8] developed dynamic model of SPIG based standalone power generation system and carried out the analysis of this system under different operating conditions in simulation as well as experimentally.

In case of induction generator, an external capacitor bank is required for supplying the reactive power which helps to build up the stator voltage. The reaction in between this capacitor bank and stator parameters is known as self excitation process which is well explained in [9–11]. Krishna et al. [12–14] proposed different methods of determining the values of the excitation capacitors and various topologies of self-excited induction generator. In case of standalone system, the system frequency and the stator voltage are unknown because they are varying with the variation of machine parameters, magnetization characteristics, speed of the rotor, type of load and the value of excitation capacitor. For this reason, the assumption of the frequency and stator voltage of SPIG is very much difficult task. The performance evaluation of SPIG can be determined with the help of steady-state per phase equivalent circuit. There are basically two ways to analyse this equivalent circuit, one is the loop impedance method and the other one is the nodal admittance method [15–18]. Loop impedance method is commonly used by researchers for the analysis of three phases or six-phase induction generator. But the loop impedance method has been proposed in this paper for finding out the maximum power delivery capability of SPIG. By using the loop impedance method, the calculation complexity can be reduced and the analysis becomes simple.

For a known capacitance, the load characteristic of SPIG is nearly same as the P-V curve for a load bus of power system [19]. It can be alternatively stated that the SPIG has maximum power transmission capability, known as critical point, which directly depends on the value of excitation capacitor. Murthy et al. [20] determined the value of excitation capacitor along with maximum power transmission capability of a wind driven SEIG. But the authors mainly focused on the wind turbine not the generator for finding out the maximum power output. Mahato et al. [21] found out the optimized value of excitation capacitor for extracting maximum power from a three-phase self-excited induction generator feeding single-phase load. Generally it is seen that at critical point, the stator voltage is much less than its rated value. That is why, to ensure the minimum pre-specified stator voltage, the machine should be operated away from its critical point. Hence, for the successful and effective operation of SPIG, it is very important to find out the critical point as well as maximum power transmission capability while maintaining the minimum pre-specified stator voltages.

Accordingly, the main contribution of this paper is to find out the critical power point and the maximum power generation capability of a SPIG for different operating conditions with the help of a simple and easy loop

impedance method. An optimization based algorithm has been formulated to determine these critical power and maximum power transmitting capability while maintaining the minimum pre-specified terminal voltage. The optimization problem has been solved very easily using Fmincon toolbox of MATLAB. The effects of capacitor, load power factor and speed on the critical power and the maximum power transmission capability have been studied. Moreover, the variation of the terminal voltage has also been analyzed with respect to the different values of capacitor and load.

This paper is sub-divided into five sections. Section – I contains introduction part, a brief literature survey and the main contribution of the paper. Section – II explains the machine modeling based on its equivalent circuit and also describes the load characteristics. The optimization problem formulation is discussed in Section – III. Section – IV describes the simulation results followed by conclusion in Section – V.

2 Modeling of SPIG and Load Characterization

Figures 1 and 2 show the schematic diagram of the six-phase induction generator (SPIG) system and the steady-state per-phase equivalent circuit of SPIG respectively in which all machine parameters including excitation capacitor

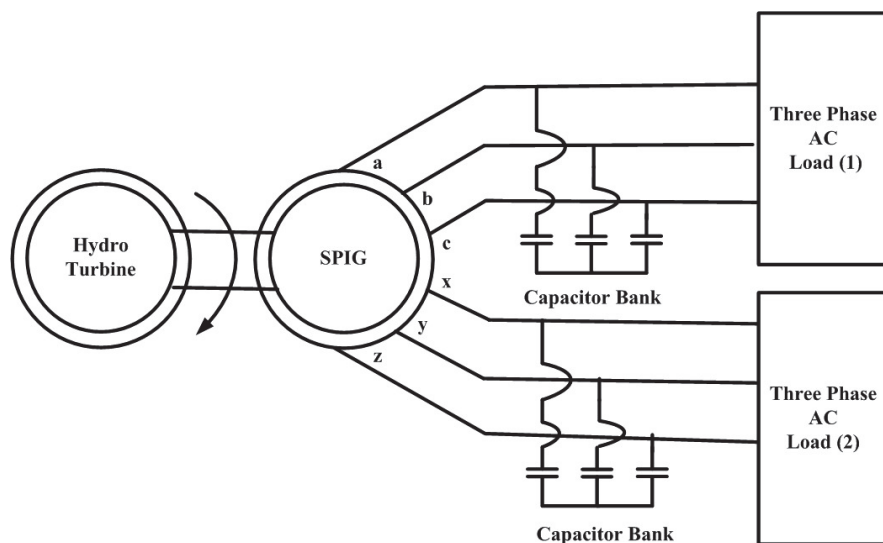


Figure 1 Schematic structure of proposed self excited six-phase induction generator.

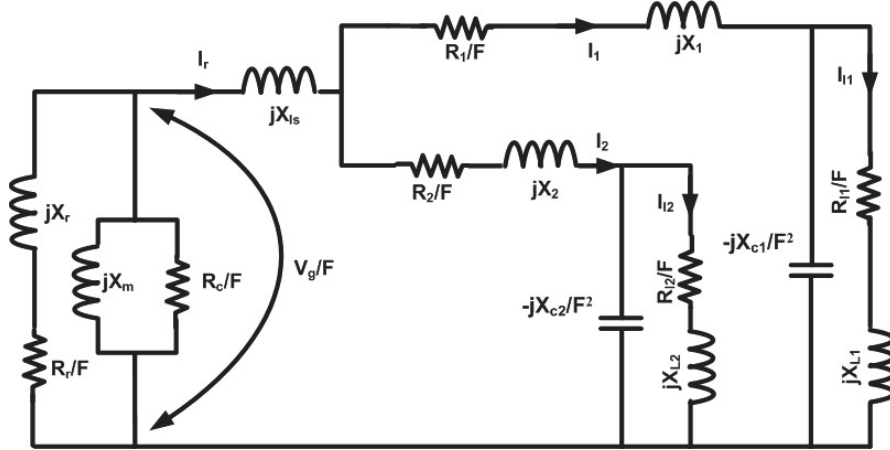


Figure 2 Per-phase equivalent circuit diagram of six-phase induction generator.

and load impedance for both windings have been shown. In Figure 2, R_{l1} , R_{l2} , X_{l1} , X_{l2} represent the stator resistances and leakage reactances respectively for both windings. R_r and X_r represent the rotor resistance and leakage reactance respectively. The core loss resistance and magnetization reactance are mentioned by R_c and X_m . The reactances of the excitation capacitances for both the windings are denoted by X_{c1} and X_{c2} . Two individual load impedances are connected in both the windings which are mentioned by Z_{l1} and Z_{l2} . F and u represent the per unit frequency and per unit speed of SPIG respectively.

All the parameters of the SPIG are constant except the magnetizing reactance, X_m as it depends on the magnetic saturation. For establishing a relation between V_g/F and X_m , the synchronous speed test is conducted on the generator. The variation between V_g/F and X_m is non-linear due to the magnetic saturation. For this system, the relation between X_m and V_g/F is expressed with the help of a third order polynomial equation [22–24].

$$\frac{V_g}{F} = -K_1 X_m^3 + K_2 X_m^2 - K_3 X_m + K_4 \quad (1)$$

where, $K_1 = 0.0002$, $K_2 = 0.0657$, $K_3 = 8.0427$, $K_4 = 550.81$.

The per phase equivalent circuit diagram of SPIG, shown in Figure 2, can be expressed in simplified form with the help of six impedances (Z_{s1} , Z_{s2} , Z_{l1} , Z_{l2} , Z_{ls} and Z_r), as presented in Figure 3. The expressions of the impedances

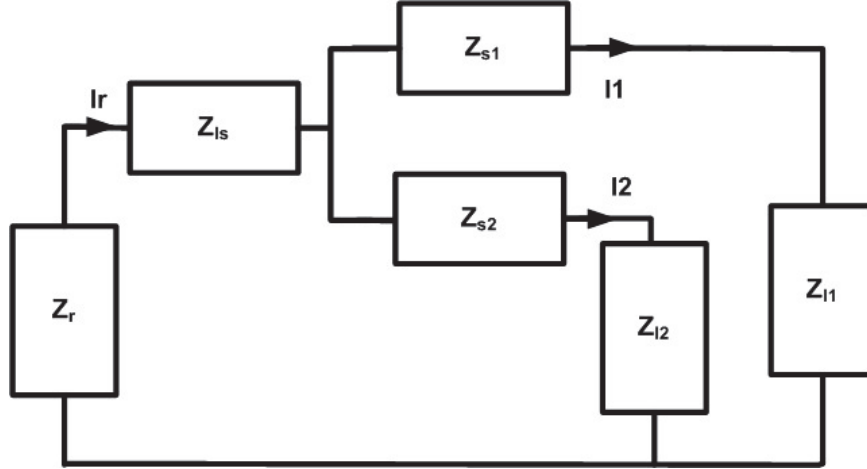


Figure 3 Simplified diagram of the equivalent circuit.

can be written as

$$Z_{s1} = \frac{R_1}{F} + jX_1 \tag{2}$$

$$Z_{s2} = \frac{R_2}{F} + jX_2 \tag{3}$$

$$Z_{l1} = \left(\frac{R_{l1}}{F} + jX_{l1} \right) \parallel \left(-\frac{jX_{c1}}{F^2} \right) \tag{4}$$

$$Z_{l2} = \left(\frac{R_{l2}}{F} + jX_{l2} \right) \parallel \left(-\frac{jX_{c2}}{F^2} \right) \tag{5}$$

$$Z_{ls} = jX_{ls} \tag{6}$$

$$Z_r = \left(jX_r + \frac{R_r}{F - u} \right) \parallel (jX_m) \parallel (R_c/F) \tag{7}$$

It is seen that for each stator winding, the stator parameters and the load impedance are connected in series and both of the series components of two windings are connected in parallel.

From Figure 3, by applying KVL, it can be written as

$$I_r (Z_r + ((Z_{s1} + Z_{l1}) \parallel (Z_{s2} + Z_{l2}))) = 0 \tag{8}$$

Since the total circuit current, I_r cannot be zero in normal operating condition, it implies that the total impedance should be zero.

$$Z_r + ((Z_{s1} + Z_{l1}) \parallel (Z_{s2} + Z_{l2})) = 0 \quad (9)$$

This impedance equation can be sub-divided in two parts, one is the real part and the other is the imaginary part.

$$Z_{real} = \text{real}(Z_r + ((Z_{s1} + Z_{l1}) \parallel (Z_{s2} + Z_{l2}))) = 0 \quad (10)$$

$$Z_{imag} = \text{imag}(Z_r + ((Z_{s1} + Z_{l1}) \parallel (Z_{s2} + Z_{l2}))) = 0 \quad (11)$$

Equation (9) is the main fundamental equation of SPIG, which should satisfy each and every operating condition. When load impedance is connected across the stator terminals, then there are total seven unknown parameters of SPIG (X_m , F , u , X_{c1} , X_{C2} , Z_{l1} and Z_{l2}). With the help of two independent Equations (10) and (11), the values of X_m and F can be solved by using a suitable iterative method after assuming the rest five unknowns (u , X_{c1} , X_{C2} , Z_{l1} and Z_{l2}). Once X_m and F are known, then the value of V_g can be evaluated easily with the help of the magnetization Equation (1). By knowing the value of V_g , the voltages, currents and power of SPIG can easily be evaluated.

The load characteristics (stator voltage with respect to output power) of SPIG can be found out by repeatedly solving the Equations (10) and (11) associated with Equation (1) for different values of load impedance and pre-assumed values of excitation capacitor and speed. Figure 4 represents the basic load characteristics of a SPIG. It is seen from this figure that, when no load (i.e., load impedance is infinite) is connected across the stator terminals, the output power is zero and the terminal voltage is at its maximum value, known as no-load voltage (V_{nl}). By reducing the load impedance gradually, it is noticed that the output power is increasing and the corresponding voltage is decreasing. This process continues until the point O is reached in the graph, which is known as critical point at which the power reaches its maximum value. Up to this point, it is the stable operating zone of SPIG. With further reduction of load impedance, the system enters to an unstable operation zone where both the voltage and power are reduced. Corresponding voltage and power of point O is known as critical voltage (V_{cr}) and critical power (P_{cr}) respectively.

At the critical point, the terminal voltage is very low as compared to the required range of the output voltage, which is highly undesirable. Due to this, a pre-specified minimum voltage (V_{min}) needs to be maintained at the time of operation of SPIG. Hence, the power transmission capability is reduced to

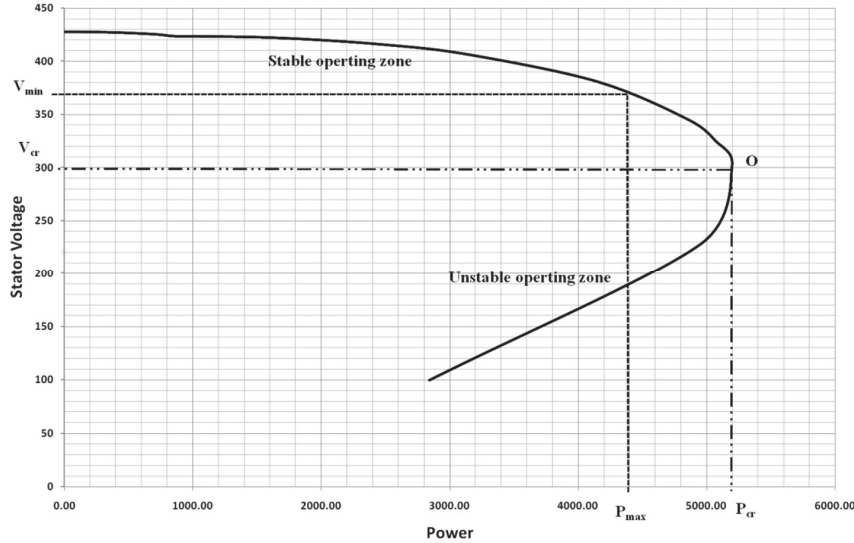


Figure 4 Stator voltage versus power characteristics of SPIG.

P_{\max} which is less than P_{cr} . The difference between V_{cr} and V_{\min} is known as voltage margin and the difference between P_{cr} and P_{\max} is known as the power margin. So for a typical and effective operation of SPIG, the amount of power transmission and corresponding voltage should be in their respective region.

3 Problem Formulation

The value of V_g can easily be obtained with the help of the magnetizing characteristics of the machine and the total impedance Equations (10) and (11). Once V_g is known, then the stator terminal voltage (V_t) can be evaluated as per the equations given below based on the equivalent circuit of the SPIG. As per the equivalent circuit of SPIG, Z_{s1} and Z_{s2} are in series with Z_{l1} and Z_{l2} respectively. Also they are parallel to each other and in series with Z_{ls} . Equation (12) is used to find out the voltage across Z_{l1} with the help of simple voltage division rule.

$$V_t = (V_g / (((Z_{s1} + Z_{l1}) \parallel (Z_{s2} + Z_{l2})) + Z_{ls})) * ((Z_{s1} + Z_{l1}) \parallel (Z_{s2} + Z_{l2})) * \left(\frac{Z_{l1}}{Z_{s1} + Z_{l1}} \right) \quad (12)$$

To satisfy the pre-specified minimum stator terminal voltage (V_{\min}), the following constraint should be maintained at the time of operation.

$$V_{\min} - V_t \leq 0 \quad (13)$$

As both of the windings are parallel to each other, the voltage V_t across the windings is same. The current passing through the individual load of both windings can be written as:

$$I_{l1} = V_t / (R_{l1} + jX_{l1}) \quad (14)$$

where, the individual load admittance can be written as

$$Y_{l1} = 1 / (R_{l1} + jX_{l1}) \quad (15)$$

So the total real power transmission capability of SPIG is given as:

$$P = 6 * I_{l1}^2 * R_{l1} \quad (16)$$

The critical power (P_{cr}) can be found out by optimizing the Equation (16) while satisfying the basic fundamental Equations (10) and (11) of the SPIG. For execution of this process, the load impedance of both windings needs to vary during the optimization process. For transmitting the maximum power (P_{max}) while maintaining the pre-specified minimum voltage (V_{\min}), the optimization process must include the Equation (13), which acts as an inequality constraint. So by assuming the values of excitation capacitance for both the windings and speed, finally the optimization problem can be written as

$$\text{Minimize } f(X) = -6 * I_{l1}^2 * R_{l1} \quad (17)$$

Subject to

$$\text{real}(Z_r + ((Z_{s1} + Z_{l1}) || (Z_{s2} + Z_{l2}))) = 0 \quad (18)$$

$$\text{imag}(Z_r + ((Z_{s1} + Z_{l1}) || (Z_{s2} + Z_{l2}))) = 0 \quad (19)$$

$$V_{\min} - V_t \leq 0 \quad (20)$$

where,

$$X = [X_m \ F \ Z_{l1} \ Z_{l2}]^T$$

This above numerical based formulated problem is solved by using Fmincon toolbox of MATLAB. This Fmincon method is used to find out

the minimum value of objective function with the help of several variables with an initial estimate. This is basically considered as a non-linear problem formulation or non-linear optimization algorithm. Here, Equation (17) is considered as the main objective function of Fmincon optimization toolbox. Equations (18), (19) and (20) are considered as non-linear constraints of this numerical based formulation problem. For execution of this Fmincon toolbox, the starting assumption, lower and upper bounds of X matrix needs to be assumed. For finding critical power (P_{cr}), minimum voltage (V_{min}) should be set to lower than critical voltage (V_{cr}) and for finding the maximum power (P_{max}), the minimum voltage (V_{min}) should be set to higher than critical voltage (V_{cr}).

4 Results Analysis and Discussions

The detailed modeling of the SPIG based system is implemented in MATLAB. All the machine parameters are given in Appendix. The developed MATLAB model is run under different operating conditions, such as, with and without pre-specified V_{min} , variation of excitation capacitor, load impedance and per unit speed. All the results obtained are explained in the following parts:

First of all, the value of critical power (P_{cr}) is derived by optimizing the Equation (17) with the help of the constrained Equations (18) and (19) while the load is purely resistive (unity power factor). Figure 5 shows the variation of the critical power with the excitation capacitance considering V_{min} as zero. It is found that when the value of excitation capacitor is low (say, 10 μ F), then P_{cr} is also very low. With the increase of the excitation capacitor, P_{cr} is increased. When the value of the excitation capacitor is 60 μ F, the critical power is high but the terminal voltage is very much reduced from its rated value. Here, the equation of the critical power is: Critical power = (41.67 * capacitance) + 4623. Hence, the slope of the critical power line is 41.67.

As the above part deals with the value of critical power, V_{min} is considered as zero or the constrained Equation (20) is neglected. But at the time of finding out the maximum power (P_{max}) for a pre-specified minimum voltage (V_{min}), the Equation (20) should be considered as one more constraint in the problem formulation of maximum power. Generally at the time of loading, the terminal voltage is little bit dropped from its rated value. In this study, the value of pre-specified minimum terminal voltage is set to five different values for this analysis. Once minimum terminal voltage is specified by

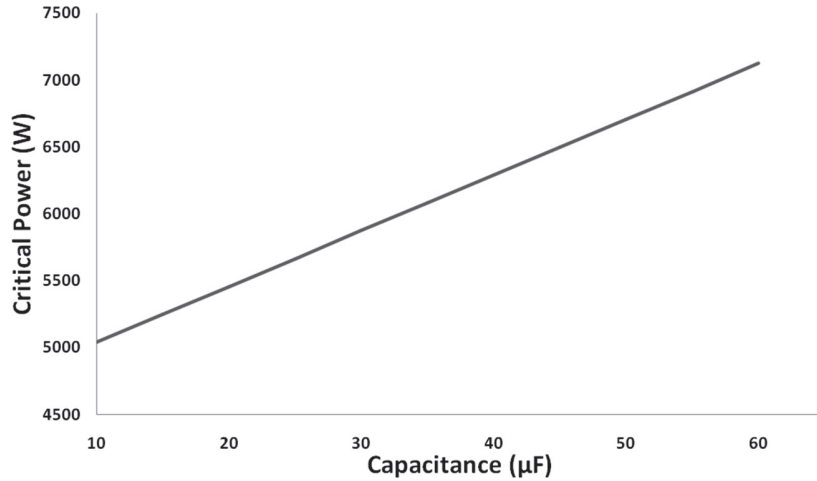


Figure 5 Critical power variation with respect to excitation capacitor.

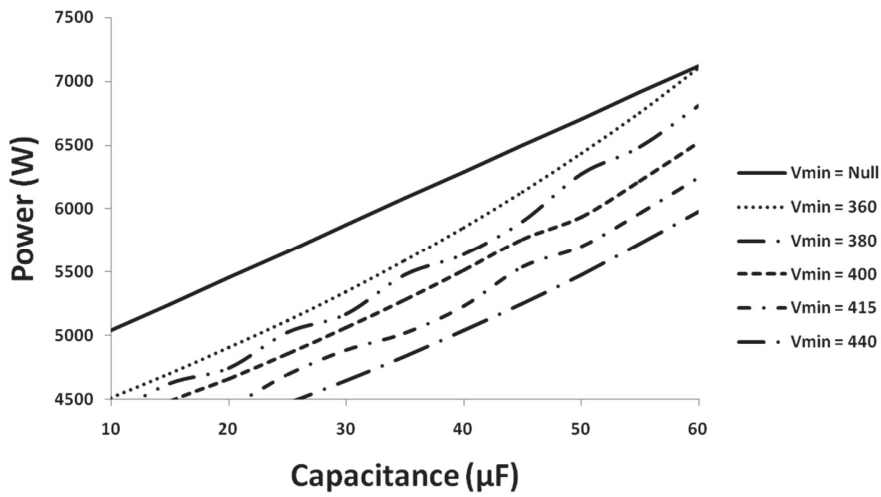


Figure 6 Critical and maximum power variation with respect to excitation capacitor for different values of V_{min} .

Equation (20) and then by varying the excitation capacitor, the maximum power delivery capability of SPIG can be determined by the optimization algorithm. From Figure 6, it is seen that when the value of V_{min} is set to lower value, then the maximum power is closed to the critical power (P_{cr}). With the increase of the pre-specified V_{min} values, the difference between the

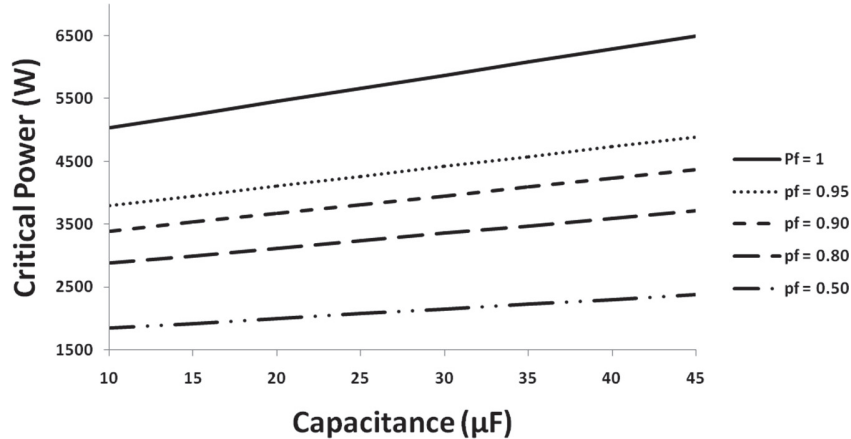


Figure 7 Critical power variation with respect to excitation capacitor for different values of load power factor.

critical power and the maximum power is increased. It is seen that maximum output power of the SPIG is approximately reached to its critical power when the minimum voltage is set to 360 V and the excitation capacitor is set to 60 μF , but when the minimum voltage is preset to 415 V, then the maximum power delivery is reduced to nearly 6 kW.

In the previous cases, for finding out the critical power, the resistive load (unity power factor) has been considered. Now, considering inductive load (lagging power factor), the variations of the critical power with change in capacitance is shown in Figure 7 for different power factors. The excitation capacitor mainly supplies the reactive power required for both the SPIG and the load. Now when the inductive load is connected, the reactive power demand by load is higher compared to the resistive load. For this reason, less amount of reactive power is available for SPIG and due to this the critical power is reduced from the unity power factor condition. It is also seen that the critical power is reduced with the reduction of power factor as the reactive power demand by the load is increased. It is clearly seen that when power factor is considered as 0.5, then the critical power is much less as compared to its rated value. For 0.9 power factor, the equation of critical power is: critical power = $(28.03 * \text{capacitance}) + 3111$. Hence, the slope is 28.03.

Figure 8 gives the variation of critical power with respect to speed variation. It is noticed that the critical power is increased with the increase in per unit speed. For 0.75 per unit speed, the equation of critical power is: critical power = $(39.68 * \text{capacitance}) + 4457$. Hence, the slope is 39.68.

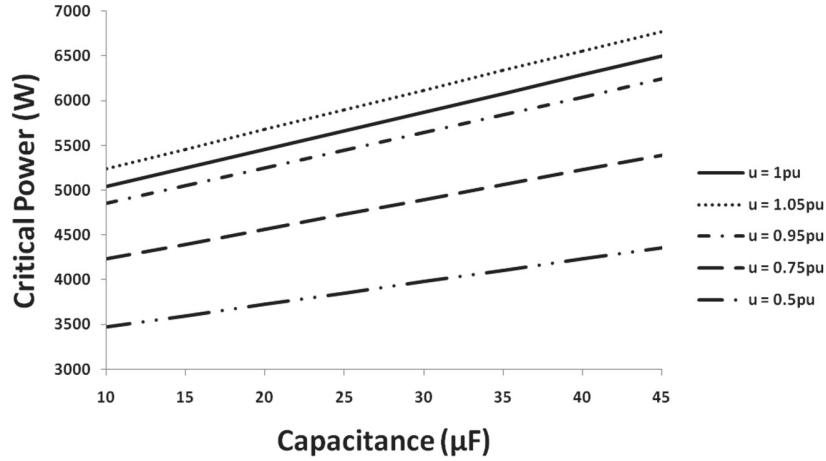


Figure 8 Critical power variation with respect to excitation capacitor for different values of per unit speed.

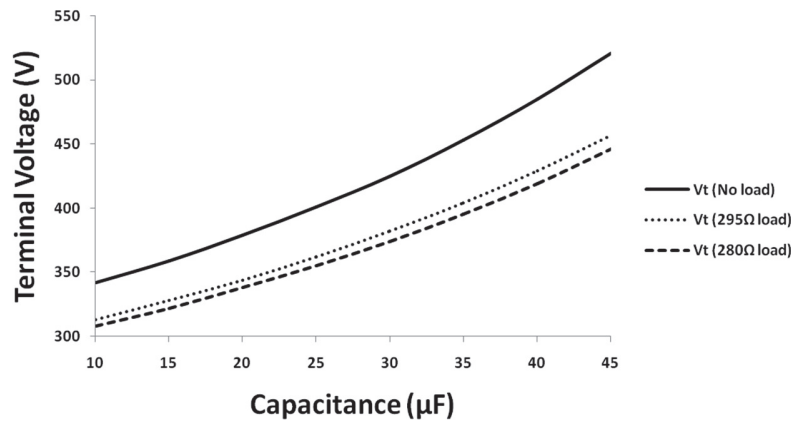


Figure 9 Terminal voltage variation with respect to excitation capacitor (with and without load).

Figure 9 presents the variation of terminal voltage with the variation of excitation capacitor for different values of load resistances. It is found that the terminal voltage increases with the increase of the capacitance. Also, the terminal voltage is reduced with the increase of load for a fixed capacitance value. From the figure, it is seen that, when SPIG is connected with excitation capacitor of $45\mu\text{F}$, the no-load terminal voltage is very high, nearly 500 V. For $35\mu\text{F}$ excitation capacitor, the no-load terminal voltage is nearly its operating

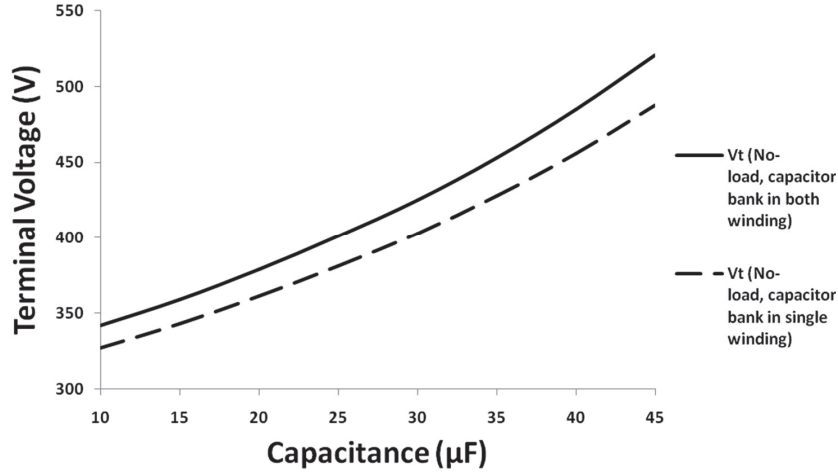


Figure 10 Terminal voltage variation with unbalanced capacitor at no load.

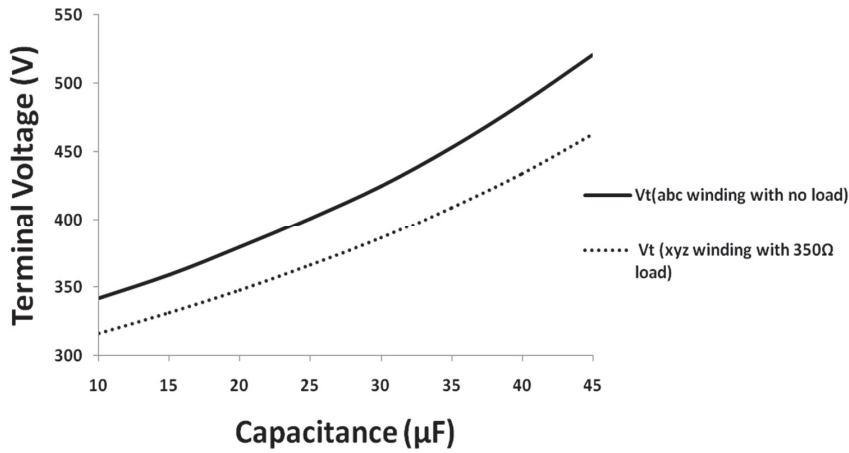


Figure 11 Terminal voltage variation with unbalanced loading.

region. When a load of 295Ω is connected across the SPIG terminals, the load terminal voltage is little bit dropped. At $35 \mu\text{F}$, the load voltage is nearly 410 V which is approximately 40 V less as compared to its no load voltage. When the load resistance is decreased to 280Ω , then the load voltage is further reduced to nearly 400 V .

Till now, for all the analyses, the excitation capacitor banks were connected in both the winding sets. Figure 10 presents the variation of the no-load

terminal voltage for the cases when the excitation capacitor bank is connected across (i) one winding set and (ii) both the winding sets. It is observed that when the both winding sets contain the capacitor bank, the operating voltage is reached with per phase capacitor of $35 \mu\text{F}$ at no-load. Now when only one excitation capacitor bank is used in any of the winding sets, then that same operating voltage is reached with per phase capacitor of $40 \mu\text{F}$.

Till now, for all the analyses, the load across both the windings is same. Figure 11 presents the variation of the terminal voltage with unbalanced loading in both windings. It is observed that voltage across the loaded winding is less compared to the winding which is at no-load.

5 Conclusions

The modeling of SPIG and loop impedance method based simple procedure to find out the maximum power transmission capability of SPIG, have been presented in this paper. An optimization based problem has been formulated while maintaining the basic fundamental equations of SPIG and the pre-specified minimum value of terminal voltage. This formulated problem has easily been solved by using Fmincon optimization toolbox of MATLAB. Depending on the pre-assumed value of V_{\min} , the critical power and the maximum power transmission capability of the SPIG are easily obtained using this same formulated problem. It is noticed that power delivery capability of SPIG is reached to its peak point when pre-specified terminal voltage is set to zero but the terminal voltage is very much reduced as compared to its rated value. For this reason, this operating region is not suitable for practical application. Hence, for a real time operation, the value of V_{\min} should not be kept as zero. From the entire analysis, it can be also noticed that the power transmission capability of SPIG not only depends on the excitation capacitor but also the load power factor and per unit speed. This type of power generating system is a promising solution for supplying power to remote location and rural areas.

Appendix

Machine Parameters

Rated power 7.2 kW, Rated voltage 415 V, Rated speed = 960 rpm.
Stator resistances ($R_1 = R_2 = 4.12 \Omega$), Stator leakage inductances (L_1 and $L_2 = 0.0216 \text{ H}$),

Rotor resistance ($R_r = 8.79 \Omega$), Rotor leakage inductance ($L_r = 0.043 \text{ H}$), Mutual inductance between two set of stator ($L_{ls} = 0.0736 \text{ H}$).

References

- [1] F. Bu, H. Xu, W. Huang, H. Liu and Y. Zhao, "Control strategy for five phase dual stator-winding induction generator DC generating system," 2015 IEEE 6th International Symposium on Power Electronics for Distributed Generation Systems (PEDG), Aachen, 2015, pp. 1–4.
- [2] K. R. M. Vijaya Chandrakala and Balamurugan, S., "Simulated annealing based optimal frequency and terminal voltage control of multi source multi area system", International Journal of Electrical Power & Energy Systems, vol. 78, pp. 823–829, 2016.
- [3] K. Kurohane, T. Senjyu, A. Yona, N. Urasaki, T. Goya, and T. Funabashi, "A hybrid smart AC and DC power system," IEEE Trans. Smart Grid, vol. I, no. 2, pp. 199–204, Sep. 2010.
- [4] P. Ch. L oh, D. Li, Y. K. Chai, and F. Blaabjerg, "Autonomous operation of hybrid micro grid with AC and DC subgrids," IEEE Trans. Power Electron., vol. 28, no. 5, pp. 2214–2223, May. 2013.
- [5] Levi E, Bojoi R, Profumo F, Williamson S. Multiphase induction motor drives – a technology status review. IET Electric Power Applications 2007; 1:489–516.
- [6] Barrero, Federico, and Mario J. Duran. "Recent advances in the design, modeling, and control of multiphase machines—Part I." IEEE Transactions on Industrial Electronics 63.1 (2016): 449–458.
- [7] Duran, Mario J., and Federico Barrero. "Recent advances in the design, modeling, and control of multiphase machines—Part II." IEEE Transactions on Industrial Electronics 63.1 (2016): 459–468.
- [8] Kamel Nounou, Khoudir Marouani, Mohamed Benbouzid, Bekheira Tabbache. Six-phase induction machine operating as a standalone self-excited induction generator. IEEE ICGE 2014, Mar 2014, Sfax, Tunisia. pp. 158–163. fhal-01023508f.
- [9] T. S. B. R. C. Bansal and D. P. Kothari, "Bibliography on the application of induction generators in non-conventional energy systems," *IEEE Trans. EC*, vol. 18, pp. 433–439, 2003.
- [10] G. Singh, "Self-excited induction generator research survey," *Power Sys. Res. (Elsevier)*, vol. 69, pp. 107–114, 2004.

- [11] D. K. A. Kheldoun, L. Refoufi, "Analysis of the self-excited induction generator steady state performance using a new efficient algorithm," *Electric Power Systems Research*, vol. 86, pp. 61–67, 2012.
- [12] Bala Murali Krishna, Vanka and Vuddanti, Sandeep. "Identification of the best topology of delta configured three phase induction generator for distributed generation through experimental investigations." *International Journal of Emerging Electric Power Systems*, vol., no., 2021, pp. 000010151520210064. <https://doi.org/10.1515/ijeeps-2021-0064>.
- [13] B. M. K. V and V. Sandeep, "Experimental Study on Different Modes of Self Excited Induction Generator Operation," 2020 2nd PhD Colloquium on Ethically Driven Innovation and Technology for Society (PhD EDITS), 2020, pp. 1–2, doi: 10.1109/PhDEDITS51180.2020.9315310.
- [14] Bala Murali Krishna, Sandeep "Design and Simulation of Current Sensor based Electronic Load Controller for Small Scale Three Phase Self Excited Induction Generator System." *International Journal of Renewable Energy Research*. Vol. 10, No. 4 (2020).
- [15] M. H. Haque, A Novel method of evaluating performance characteristics of a self-excited induction generator", *IEEE Trans. On Energy Conversion*, Vol. 24, No. 2, 2009, pp. 358–365.
- [16] R. C. Bansal, "Three-phase self-excited induction generators: An overview", *IEEE Transactions on Energy Conversion*, Vol. 20, No. 2, 2005, pp. 292–299.
- [17] M. G. Simoes and F. A. Farret, "Renewable energy systems – design and analysis with induction generators", CRC Press, 2004.
- [18] T. F. Chan, "Steady-state analysis of self-excited induction generators", *IEEE Transactions on Energy Conversion*, Vol. 9, No. 2, 1994, pp. 288–296.
- [19] C. W. Taylor, "Power system voltage stability", McGraw-Hill, New York, 1994.
- [20] S. S. Murthy and R. K. Ahuja, "Capacitive VAR and MPPT estimation of wind driven self excited induction generators for decentralized power generation using MATLAB graphical user interface based methodology" *IEEE International Conference of Power Electronics, Drives and Energy Systems*, Bengaluru, India, 2012.
- [21] S. N. Mahato, S. P. Singh and M. P. Sharma, "Capacitors required for maximum power of s self-excited single-phase induction generator using a three-phase machine", *IEEE Transactions on Energy Conversion*, Vol. 23, No. 2, 2008, pp. 372–381.

- [22] Singh GK, Senthil Kumar A, Saini RP. Performance evaluation of series compensated self-excited six-phase induction generator for stand-alone renewable energy generation. *Energy* 2010; 35:288–97.
- [23] Singh GK, Senthil Kumar A, Saini RP. “Selection of capacitance for self-excited six-phase induction generator for stand-alone renewable energy generation” *Energy*, Volume 35, Issue 8, 2010, Pages 3273–3283, ISSN 0360-5442.
- [24] Singh GK, Senthil Kumar A, Saini RP. Performance analysis of a simple shunt and series compensated six-phase self-excited induction generator for stand-alone renewable energy generation. *Energy Conversion and Management*, Volume 52, Issue 3, 2011, Pages 1688–1699, ISSN 0196-8904.

Biographies



Saikat Ghosh received the bachelor’s degree in Electrical Engineering from College of Engineering and Management, Kolaghat in 2015, the master’s degree in Electrical Engineering from National Institute of Technology, Arunachal Pradesh in 2017. Currently, he is a Research Scholar in Electrical Engineering Department, National Institute of Technology, Durgapur. His research areas include power electronics and drives, multi-phase induction machine, renewable energy etc.



S. N. Mahato received the B.E. degree in electrical engineering in 1992 and the M.Tech. degree in 2002 from the National Institute of Technology, Durgapur, India. He received Ph.D. degree from Indian Institute of Technology, Roorkee, in 2008. Currently, he is a professor in the Department of Electrical Engineering, National Institute of Technology, Durgapur. His current research interests include application of induction generator for generating power from nonconventional energy sources.

